Full Paper
Journal of Nano Materials Impact 2026, 02 (02) 30-37

Theoretical Investigation of Solvent and Temperature Effects on Photoinduced Interfacial Charge Transfer Rate at the Ag-NTCDA Nanoscale System

Taif Saad Al Maadhede
Department of Renewable Energy, College of Energy and Environmental Science, Al-Karkh University of science, Baghdad, Iraq.

Abstract

In this study, charge transfer (CT) at the metal (Ag)and 1, 4, 5, 8-Naphthalenetetracarboxylic dianhydride (NTCDA) was investigated using a non-adiabatic system and quantum transfer theory. The CT rate expression used to estimate the CT rate is assumed to be a continuum level for the Ag-NTCDA interface. The reorganization energy, driving force, and CT rate of the Ag - NTCDA system was calculated based on quantum theory. This study examines the effects of reorganization energy, electronic coupling, and temperature on the CT rate. The results indicate that the solvent polarity and dielectric constant influence the reorganization energy, and consequently, the CT rate. As the reorganization energy decreases, the CT rate increases, and vice versa. The electronic coupling between the Ag state and NTCDA molecular state has the strongest influence on the rate. Increasing the electronic coupling produces a quadratic enhancement of the charge transfer, consistent with the nonadiabatic CT regime. Temperature effects are also observed with increasing from 305 K to 315 K, leading to a (13-19) % CT enhancement, depending on the solvent environment. These results demonstrate that the charge transfer rate at the Ag - NTCDA interface is strongly governing it by the interplay among reorganization energy electronic coupling, temperature and solvent effect.

Keyword: Ag-NTCDA interface • charge transfer (CT) • electronic coupling • reorganization energy.

Downloaded from https://nanomatimp.uomustansiriyah.edu.iq/

Introduction

The Metal-molecule interfaces are crucial to investigate charge transfer CT dynamics that dictate charge injection, separation and transport in molecularly electronic and photoactive systems. Factors such as the electronic interaction between molecular and metallic states, energy alignment of donor and acceptor levels, nuclear rearrangement and polarization effects from the environment determine how fast or slow the CT occur via these interfaces. Therefore, a correct description and control of the charge-transfer dynamics in nanoscale systems requires a comprehensive understanding of such parameters[1, 2]

Because they combine localized molecular electronic states with the quasi-continuous electronic states of metallic substrates, organic molecules adsorbed on noble-metal surfaces offer useful model systems for investigating interfacial electron transfer processes. The Ag–NTCDA interface is an example of a metal–organic system in which 1, 4, 5, 8-naphthalene-tetracarboxylic dianhydride (NTCDA) acts as an electron-accepting molecule through its empty molecular states, whereas the silver substrate provides a variety of electronic states close to the Fermi level. Numerous theoretical and experimental investigations of the interaction between NTCDA and Ag surfaces have demonstrated the importance of interfacial charge redistribution and molecule–substrate coupling in defining the electrical characteristics of metal–organic interfaces[3-5].

Quantum mechanical and semiclassical techniques have been applied to improve the theoretical foundation of electron transfer processes. Marcu's theory, which links the transfer rate to elements such as electronic coupling, the driving power of the reaction, and reorganization energy, offers a basic foundation for understanding nonadiabatic electron-transfer processes, this phenomenon occurs when the electron coupling strength between the donor and the acceptor is very weak; this means that the electronic state changes as the electron is rapidly lost between the potential energy surfaces.

According to the Marcus–Levich model, the reorganization process is influenced by nuclear and environmental polarization coordinates, and the CT is defined by variations in the energy gap between the initial and final electronic states. The Franck-Condon weighted density of accepting states, which is produced by these oscillations, establishes the likelihood of CT[6]. Because metallic electrodes provide a quasi-continuous spectrum of electronic states rather than a single discrete energy level, the electron-transfer process at metal–molecule interfaces differ from that in traditional donor–acceptor systems. The Fermi golden rule is used to represent the transition probability in the nonadiabatic weak-coupling scenario, which is computed using time-dependent quantum mechanics (QM). The density of accessible

***Address for correspondence:** Taif Saad Al Maadhede, Department of Renewable Energy, College of Energy and Environmental Science, Al-Karkh University of science, Baghdad, Iraq.
E-mail: hudasaadi@kus.edu.iq
ORCID: https://orcid.org/0000-0002-6963-9385

This is an open-access journal, and articles are distributed under the terms of the Creative Commons Attribution License (CC-BY) 4.0 License, which allows others to use, distribute, and reproduce in any medium for noncommercial purposes, as long as the original work is cited properly.

Info:
Submitted: 11 May 2026; **Revised:** 19 June 2026;
Accepted: 03 July 2026; **Published:** 15 Aug. 2026.
https://doi.org/10.71109/nmi.2026.2.2.38

Copyright © 2026. This work licensed under a Creative Commons Attribution Noncommercial 4.0 International License.

accepting states and the electronic coupling matrix element between the molecular and metallic states affect the resulting rate of CT[7, 8]. When assessing electron transfer kinetics, the temperature effects must be considered using the Fermi–Dirac distribution ($F_{(E)} = 1/1 + exp^{E/k_BT}$) because the electronic states of the metal electrode are thermally filled[9].

By altering the reorganization energy linked to charge redistribution, the solvent environment significantly affects the electron transfer kinetics. According to dielectric continuum models, the dielectric constant, refractive index, and geometric parameters defining the molecular–electrode arrangement all influence the solvent contribution to the reorganization energy[10]. As a result, changes in solvent properties can affect the driving force and activation energy of the electron transfer process by changing the stability of both the initial and final electronic states[10].

The influences of solvent on CT reactions have been analyzed according Marcu's theory, Pekar factor (solvent polarity) and dielectric constant response are important determines of CT reaction and the value of reorganization between driving force, reorganization energy and CT rate, making it a good tool for energy[11]. In addition, based on Marcu's theory predicts a quantitative relationship describing CT processes in both condensed-phase and nanoscale systems[6, 12]. While metal–organic interfaces have been well-studied, the combined roles of solvent environment and temperature on interfacial CT kinetics remains insufficiently understood.

This study offers a theoretical analysis of photoinduced CT at the Ag–NTCDA interface using a nonadiabatic metal–molecule framework in conjunction with Marcus–Levich theory. The reorganization energy, driving force energy, and electron-transfer rate constant were evaluated by considering the electronic coupling between the metallic and molecular states, Franck–Condon weighted density of accepting states, solvent effects, and temperature-dependent occupation of metallic states[13].

This study systematically investigates how varying solvent environments and temperatures affect electron transfer kinetics to elucidate the relationship between solvent properties, energetic parameters, and CT behavior at the Ag–NTCDA interface.

Theory

It can be considered a heterogeneous interface formed between generic metallic electrode M possessing a quasi-continuous manifold of electronic states close to the Fermi level and a molecular species D in acceptor, whose electronic state is localized at the interfacial region, as in the standard two-state treatment of interfacial CT. The composite electronic wave function of the coupled *M/D* system is expanded over a complete, orthonormal set of basis states χ_k[14]:

$$|\psi_{\mathrm{M-D}}(t)\rangle = \sum_{k=0}^{\infty} A_k\,(t)|\chi_k\rangle e^{-i\frac{E_k t}{\hbar}} \quad \text{... (1)}$$

where A_k is the time-dependent expansion coefficient of the basis state $|\chi_k\rangle$ and E_k is the corresponding eigenenergy. Following an Anderson-type partition of the interfacial Hamiltonian, the total Hamiltonian of the coupled system is written as[15]:

$$\hat{H} = \hat{H}_M + \hat{H}_D + \hat{H}_{M/D} \quad \text{... (2)}$$

where $\hat{H}_M$ and $\hat{H}_D$ are the unperturbed Hamiltonians of the isolated electrode and molecule, respectively, and $\hat{H}_{M/D}$ is the interfacial coupling (tunneling) Hamiltonian that mediates charge exchange across the contact region. The stationary eigenvalue problem for the composite system follows directly[14]

$$\hat{H}\,|\psi_{\mathrm{M/D}}\rangle = \hat{H}_M + \hat{H}_{\mathrm{M/D}} + \hat{H}_{\mathrm{M/D}})|\psi_{\mathrm{M/D}}\rangle \quad \text{... (3)}$$

Inserting Eq (2) into the time dependent Schrodinger equation:

$$i\hbar\frac{d}{dt}|\psi_{\mathrm{M/D}}\rangle = (\hat{H}_M + \hat{H}_D + \hat{H}_{\mathrm{M/D}})\ |\psi_{\mathrm{M/D}}\rangle \quad \text{... (4)}$$

Substituting expansion (1) into equation (4) and projecting onto the basis set yields the equation of motion for coefficient $A_k(t)$.

$$i\hbar\frac{\partial}{\partial t}A_k(t) = \sum_{k=o}^{\infty} A_k(t)\ \hat{H}_{\mathrm{M/D}}e^{-\frac{i(E_M - E_{D)t}}{\hbar}} \quad \text{... (5)}$$

The probability that a charge initially localized on M is found on D after a time t is obtained by summing the square coefficient over the accessible final state[16].

$$P(t \to \infty) = \sum_{k}^{n} |A_k(t)|^2 \quad \text{... (6)}$$

Integrating Eq. (5) to first order in the coupling (weak coupling/perturbative limit) yields an explicit time dependence of the transition probability as follows:

$$P_n = \sum_{k}^{n} |A_k(t)|^2 = \left|B_{\mathrm{M/D}}\right|^2 \hbar^{-2}\left(\frac{e^{-\frac{i(E_M - E_{D)t}}{\hbar}} - 1}{\frac{(E_M - E_{D)}}{\hbar}}\right)^2 \quad \text{... (7)}$$

where $B_{\mathrm{M/D}} = \langle\chi_M|\hat{H}_{\mathrm{M/D}}|\chi_D\rangle$ is the electronic coupling matrix element between the metal and molecular state[17]. Writing $\hbar\omega_{\mathrm{M/D}} = E_M - E_D$, Eq. (7) reduces to:

$$P_n = \left|B_{\mathrm{M/D}}\right|^2 \hbar^{-2}\left(\frac{e^{-\frac{i\omega_{M/D}t}{\hbar}} - 1}{\omega_{\mathrm{M/D}}}\right)^2 \quad \text{... (8)}$$

Using the identity $|e^{ix} - 1|^2 = 4sin^2(\frac{x}{2})$ [18] together with the long-time $\lim_{t\to\infty}\left(\frac{sin^2(xt)}{x^2}\right) = \pi t\delta(x)$[18, 19], Eq. (8) can be written compactly as:

$$P_n = \left|B_{\mathrm{M/D}}\right|^2 \hbar^{-2}\delta(E_M - E_{D)} \quad \text{... (9)}$$

The instantaneous transition rate follows from the time derivative of Eq. (9), in the spirit of the Fermi golden rule.

$$\mathcal{R}_{B_{\mathrm{M/D}}} = 2\pi\left|B_{\mathrm{M/D}}\right|^2 \hbar^{-1}\delta(E_M - E_{D)} \quad \text{... (10)}$$

Downloaded from https://nanomatimp.uomustansiriyah.edu.iq/

Copyright © 2026. This work licensed under a Creative Commons Attribution Noncommercial 4.0 International License.

Because the metal electrode possesses a quasi-continuum of states at the Fermi level, the total transfer rate n is obtained by integrating Eq. (10) against the density of acceptor states $\wp(E)$:

$$\mathcal{R}_{B_{M/D}} = 2\pi \left|B_{\frac{M}{D}}\right|^2 \hbar^{-1} \int \wp(E)\, \delta(E_M - E_{D)}\, dE \quad \text{... (11)}$$

To define $\wp(E)$, we adopt the classical framework proposed by Marcus and Levich. In this model, the energy gap between the M and D electronic configurations is influenced by a continuous classical reorganization coordinate. This coordinate symbolizes the collective response of the surrounding lattice and solvent polarization to the transferred charge. Because this coordinate is linearly coupled to the reaction and thermally populated, the instantaneous energy gap exhibits fluctuations that follow a Gaussian distribution. This distribution is centered on the equilibrium driving force, with its variance determined by the thermal energy k_BT ,where k_B is the Boltzman constant and T is temperature, and the reorganization energy ($\mathfrak{H}$)of the pair. Consequently, the Franck–Condon-weighted density of accepting states assumes the well-known Gaussian (Marcus–Levich) form[20]:

$$\wp(E) = (4\pi\mathfrak{H}k_BT)^{\frac{-1}{2}} \exp\left(\frac{-(\mathfrak{H} + \Delta V)^2}{4\mathfrak{H}k_BT}\right) \quad \text{... (12)}$$

where $\mathfrak{H}$ is the reorganization energy of the system, k_B is the Boltzmann constant, T is the temperature and ΔV is the potential difference across the interface, which is related to the reaction driving force ΔG° by[21]:

$$\Delta V = \Delta G^\circ - E \quad \text{... (13)}$$

Substituting Eq. (12) and Eq. (11) gives:

$$\mathcal{R}_{\frac{M}{D}} = 2\pi\hbar^{-1}\left|B_{\frac{M}{D}}\right|^2 (4\pi\mathfrak{H}k_BT)^{\frac{-1}{2}} \int \exp\left(\frac{-(\mathfrak{H} + \Delta V)^2}{4\mathfrak{H}k_BT}\right) \delta(E_M - E_{D)}\, dE \quad \text{... (14)}$$

As only electrode states below the Fermi level are occupied, it is necessary to weight the integrand by the Fermi–Dirac occupation factor[22].

$$F_{(E)} = \frac{1}{1 + exp^{\frac{E}{k_BT}}} \quad \text{... (15)}$$

Inserting $F_{(E)}$and Eq. (13) in to Eq. (14) becomes;

$$\mathcal{R}_{\frac{M}{D}} = 2\pi\hbar^{-1}\left|B_{\frac{M}{D}}\right|^2 (4\pi\mathfrak{H}k_BT)^{\frac{-1}{2}} \int \exp\left(\frac{-(\mathfrak{H} + \Delta G^\circ - E)^2}{4\mathfrak{H}k_BT} F_{(E)} \delta(E_M - E_{D)}\, dE\right) \quad \text{... (16)}$$

Simplify expression in Eq. (16) to give:

$$\mathcal{R}_{\frac{M}{D}} = 2\pi\hbar^{-1}\left|B_{\frac{M}{D}}\right|^2 (4\pi\mathfrak{H}k_BT)^{\frac{-1}{2}} \int \exp\left(\frac{-(\mathfrak{H} + \Delta G^\circ - E)^2}{4\mathfrak{H}k_BT} \frac{1}{1 + exp^{\frac{E}{k_BT}}} \delta(E_M - E_{D)}\, dE\right) \quad \text{... (17)}$$

Performing energy integration using the δ function and expanding the resulting Gaussian- fermi product to second order in k_BT valid $\mathfrak{H} \gg k_BT$ for yields the following close from expression for the temperature dependent transfer rate:

$$\mathcal{R}_{\frac{M}{D}} = 2\pi\hbar^{-1}\left|B_{\frac{M}{D}}\right|^2 (4\pi\mathfrak{H}k_BT)^{\frac{-1}{2}} \exp - \frac{\mathfrak{H}}{4k_BT} \times \left[1 - \frac{\pi^2 k_BT}{16\mathfrak{H}}\right] \quad \text{... (18)}$$

However, the reorganization energy associated with CT between the metal electrode and the molecular acceptor across the interfacial dielectric medium is estimated from the dielectric continuum theory as follows[23]:

$$\mathfrak{H} = \frac{e^2}{8\pi\varepsilon_o}\left(\frac{1}{n^2} - \frac{1}{\varepsilon}\right)\left(\frac{1}{r_D} - \frac{1}{2D}\right) \quad \text{... (19)}$$

Here, e represents the electron charge, while ε_o denotes the vacuum permittivity, and ε is the static dielectric constant of the surrounding medium. The refractive index of the medium is indicated by n, D refers to the separation between the molecular acceptor and the electrode surface (D= $r_{NTCDA} + r_{Ag}$), and r_D is the effective radius of the molecule. The effective radius is estimated based on the molecular volume as follows[24]:

$$r_D = \left(\frac{3M}{4\pi N\rho}\right)^{\frac{1}{3}} \quad \text{... (20)}$$

where M, N *and* ρ are the molecular weight, Avogadro's number, and mass density of *D*, respectively.

On the other hand, the theoretical driving force for charge transfer, ΔG°, is supplied by the excess energy deposited in the molecule upon photon absorption, offset by the reorganization energy required to reach the transition configuration[25].

$$\Delta G^\circ = E_{abs} - \mathfrak{H} \quad \text{... (21)}$$

where $E_{abs} = hf = hc/\lambda$ is the absorption energy read from the molecular absorption spectrum, h is Planck's constant, c is the speed of light, and λ is the absorption wavelength.

Results and Discussion

The quantum CT rate is a crucial parameter for assessing the efficiency of CT processes in systems, as it elucidates the nature and behavior of the CT between the donor and acceptor. This study employed the quantum Marcus theory model to investigate the CT in the Ag–NTCDA system, where the silver (Ag) surface served as the charge donor and the NTCDA molecule acted as the charge acceptor. It was assumed that the energy levels in the system remained continuous during the CT process.

Theoretical calculations were conducted to ascertain the CT rate between Ag and the organic molecule (NTCDA) in the presence of five different solvents: 1,2-dimethoxyethane, N-methyl-2-pyrrolidone (NMP), N, N-dimethylformamide (DMF), acetone, and acetonitrile.

These calculations were based on a model of CT between the donor and acceptor using MATLAB software. The CT rate was determined based on a set of parameters influencing the process, including the reorganization energy ($\mathfrak{H}$ eV), charge coupling coefficient (eV/state), driving force for the transfer process (ΔG°), and effect of temperature (T).

The reorganization energy $\mathfrak{H}$ (eV)) was computed using Equation (19), which is a function of the physical properties of the system. These properties include the radii of the donor and acceptor, the distance between them, and the dielectric constant and refractive index of the solvent.

Downloaded from https://nanomatimp.uomustansiriyah.edu.iq/

Copyright © 2026. This work licensed under a Creative Commons Attribution Noncommercial 4.0 International License.

Equation (20), which is based on the molecular weight (107.868 g mol⁻¹) and density (10.50 g cm⁻³) of Ag [26], was used to calculate the radii of the silver (Ag) metal, Ag (1.59 Å) It effect on reorganization energy, the reorganization energy decreases the reorganization energy will be increases and vice versa, and NTCDA molecules. **Table 1** displays the molecular weight and density of the NTCDA molecule. The refractive index and dielectric constant of the solvents were also considered. The reorganization energies of the systems in the different solvents, as indicated in **Table 2**, were determined using these parameters, and the reorganization energy findings are shown in **Table 3**.

Table 1. The general properties of NTCDA[26].

CAS	81-30-1
Molecular Formula	$C_{14}H_4O_6$
Molar Mass g/mol	268.178
Density (g/cm^3)	1.8
Radii (cm)	3.8948×10^{-8}
Index of Refraction	1.782
Ionization energy	8 eV
Electron affinity	4 eV
Flash Point	280.4±26.8 °C

Table 2. Physical properties of the solvents used in the Ag–NTCDA system[26].

Full Solvent Name	Abbreviation	Molecular Formula	Dielectric Constant, ε	Refractive Index, n
1,2-Dimethoxyethane	DME	$C_4H_{10}O_2$	7.20	1.379
N-Methyl-2-pyrrolidone	NMP	C_5H_9NO	32.1	1.4680
N,N-Dimethylformamide	DMF	C_3H_7NO	36.7	1.430
Acetone (Propan-2-one)	ACE	C_3H_6O	20.6	1.3588
Acetonitrile	ACN	CH_3CN	35.9	1.344

Table 3. Calculated solvent reorganization energies $\mathfrak{H}$ (eV) for CT in the Ag–NTCDA system[27].

(Solvent)	n	ε	$\frac{1}{n^2}$	$\frac{1}{\varepsilon}$	$\Delta = \frac{1}{n^2} - \frac{1}{\varepsilon}$	$\mathfrak{H}$ (eV)
DME	1.3790	7.2	0.5259	0.1389	0.3870	0.462
NMP	1.4680	32.1	0.4640	0.0312	0.4329	0.517
DMF	1.4300	36.7	0.4890	0.0272	0.4618	0.551
ACE	1.3588	20.6	0.5416	0.0485	0.4931	0.588
ACN	1.3440	35.9	0.5536	0.0279	0.5258	0.627

According to Equation (19), the reorganization energy ($\mathfrak{H}$ eV) increases steadily from 0.462 eV in DME to 0.627 eV in ACN (**Table 3**). Instead of being exclusively reliant on ε or n, this pattern is consistent with the Picard coefficient ($\frac{1}{n^2} - \frac{1}{\varepsilon}$). Aprotic polar solvent, such as ACN, require more energy to undergo rearrangement than solvents with similar optical and dielectric permittivity's, such as DME. The fluctuation of $\mathfrak{H}$ with the solvent is solely due to its polarization, because the geometric term in Equation (19) remains constant for a given diameter and distance[28]. The reorganization energy for solvents was increased with increases dielectric constant of solvents, this agrees with experimental results for same solvents with Au metal contact with Ru dye molecule in literature[29].

The order solvents (DME > NMP > DMF > ACE > ACN) were determined entirely by the value of reorganization energy. When calculating the ratio $\mathcal{R}_{\frac{M}{D}}$(DME)/$\mathcal{R}_{\frac{M}{D}}$(ACN), this ratio consistently approximated 5.6 at 305 K, irrespective of $\left|B_{\frac{M}{D}}\right|^2$. Although DMF and ACN possess close dielectric constants (36.7 and 35.9, respectively), their refractive index indices differ (1.430 and 1.344), leading to significantly different values of reorganization energy and CT rate.

Equation (21) was used to calculate the average driving force for the CT process at constant reorganization energy, represented as ΔG° (in eV). This computation considers both the previously calculated constant reorganization energy and the variety absorption energy ($E_{abs.}$). **Table 4** provides a thorough breakdown of the driving-force calculations for the Ag–NTCDA system in various solvents.

Table 4. Results of theoretical driving force energy (ΔG° eV) calculations for the NTCDA molecule in various solvent media at constant reorganization energy.

Wave length λ (nm)	Absorption energy (eV)	DME	NMP	DMF	ACE	ACN
250	4.959	4.498	4.443	4.408	4.371	4.332
300	4.133	3.671	3.616	3.582	3.545	3.506
350	3.542	3.081	3.026	2.992	2.954	2.915
400	3.100	2.638	2.583	2.549	2.511	2.472
450	2.755	2.294	2.239	2.204	2.167	2.128
500	2.480	2.018	1.963	1.929	1.891	1.852
550	2.254	1.793	1.738	1.703	1.666	1.627
600	2.066	1.605	1.550	1.516	1.478	1.439

Table 4 shows that when the wavelength decreases and the absorption energy increases, the driving force energy (ΔG°) for the system increases, and vice versa. The structure of the material, the properties of the Highest Occupied Molecular Orbital HOMO and Lowest Occupied Molecular Orbital LUMO energy levels for NTCDA, and the energy levels at the Fermi level for Ag metal all affect the potential at the interface.

Following the determination of the reorganization energy, driving force, and electronic coupling coefficient $B_{\frac{M}{D}}$= (0.25, 0.5, 0.75, 1, 1.25, 1.5, 1.75, 2) × 10^{-3} eV the CT rate $\mathcal{R}_{\frac{M}{D}}$ (s^{-1}) for the Ag–NTCDA system was computed using Equation (18). These calculations were conducted at temperatures of 305 and 315 K using MATLAB to examine the impact of temperature on the CT efficiency. The CT rates in the presence of various solvents were obtained, and the results are displayed in **Table 5** and **Figure 1** for 305 K and in **Table 6** and **Figure 2** for 315, respectively.

Table 5. Calculated CT rate constants $\mathcal{R}_{\frac{M}{D}}$ (s^{-1}) for the Ag–NTCDA system in different solvent media at 305 K.

$\left\|B_{\frac{M}{D}}\right\|$ (eV)	DME	NMP	DMF	ACE	ACN
0.25×10^{-3}	1.825×10^{7}	1.029×10^{7}	7.194×10^{6}	4.887×10^{6}	3.272×10^{6}
0.50×10^{-3}	7.300×10^{7}	4.114×10^{7}	2.878×10^{7}	1.955×10^{7}	1.309×10^{7}
0.75×10^{-3}	1.643×10^{8}	9.257×10^{7}	6.475×10^{7}	4.399×10^{7}	2.945×10^{7}
1.00×10^{-3}	2.920×10^{8}	1.646×10^{8}	1.151×10^{8}	7.820×10^{7}	5.235×10^{7}
1.25×10^{-3}	4.563×10^{8}	2.571×10^{8}	1.799×10^{8}	1.222×10^{8}	8.180×10^{7}
1.50×10^{-3}	6.570×10^{8}	3.703×10^{8}	2.590×10^{8}	1.759×10^{8}	1.178×10^{8}
1.75×10^{-3}	8.943×10^{8}	5.040×10^{8}	3.525×10^{8}	2.395×10^{8}	1.603×10^{8}
2.00×10^{-3}	1.168×10^{9}	6.583×10^{8}	4.604×10^{8}	3.128×10^{8}	2.094×10^{8}

Downloaded from https://nanomatimp.uomustansiriyah.edu.iq/

Copyright © 2026. This work licensed under a Creative Commons Attribution Noncommercial 4.0 International License.

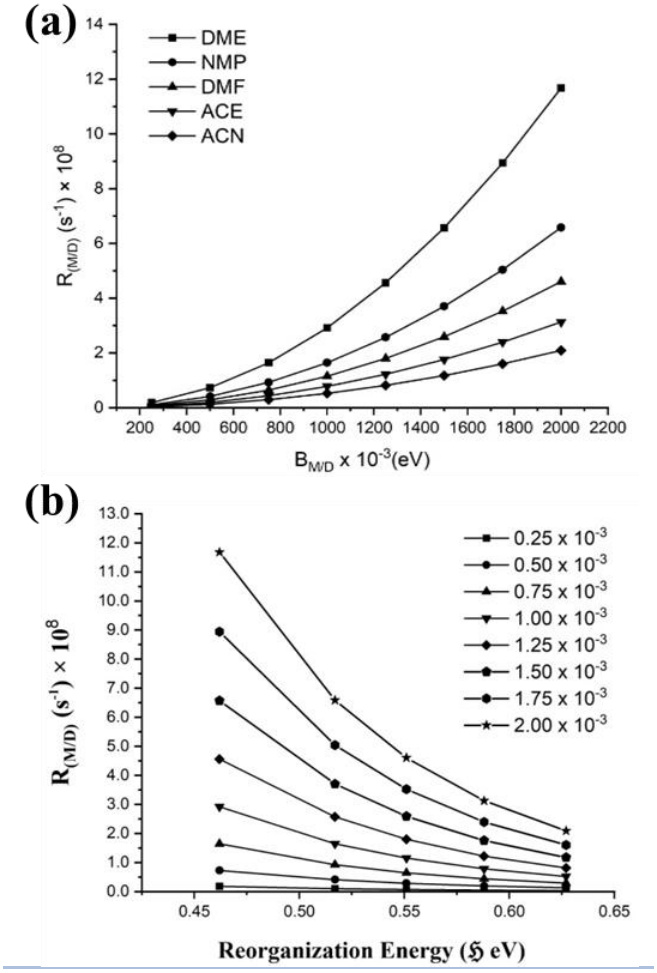


Figure 1. Behaviour of charge transfer Rate Constants $\mathcal{R}_{\frac{M}{D}}$ (s^{-1}) for the Ag–NTCDA System as function of strength coupling (a), and reorganization energy (b).

Table 6. Calculated CT rate constants $\mathcal{R}_{\frac{M}{D}}$ (s^{-1}) for the Ag–NTCDA system in different solvent media at 315 K.

$\left\|B_{\frac{M}{D}}\right\|$(eV)	DME	NMP	DMF	ACE	ACN
0.25×10^{-3}	2.062×10^{7}	1.182×10^{7}	8.352×10^{6}	5.739×10^{6}	3.887×10^{6}
0.50×10^{-3}	8.248×10^{7}	4.727×10^{7}	3.341×10^{7}	2.295×10^{7}	1.555×10^{7}
0.75×10^{-3}	1.856×10^{8}	1.063×10^{8}	7.517×10^{7}	5.165×10^{7}	3.499×10^{7}
1.00×10^{-3}	3.299×10^{8}	1.891×10^{8}	1.336×10^{7}	9.182×10^{7}	6.220×10^{7}
1.25×10^{-3}	5.155×10^{8}	2.954×10^{8}	2.088×10^{8}	1.435×10^{8}	9.719×10^{7}
1.50×10^{-3}	7.423×10^{8}	4.254×10^{8}	3.007×10^{8}	2.066×10^{8}	1.399×10^{8}
1.75×10^{-3}	1.010×10^{9}	5.790×10^{8}	4.093×10^{8}	2.812×10^{8}	1.905×10^{8}
2.00×10^{-3}	1.320×10^{9}	7.563×10^{8}	5.345×10^{8}	3.673×10^{8}	2.488×10^{8}

The results of charge transfer rate in tables (5) and (6) together figures (1) and (2) in a with strength coupling and reorganization energy in b show the charge transfer rate increases with decreases in reorganization energy while the charge transfer rate increases with increases strength coupling and vice versa. However, the results in many experimental data indicates that DMF solvent was suitable solvent with NTCDA contact with Ag[30, 31], that's agree with results in **Table 5** and **Table 6**.

A comparison of $\mathcal{R}_{\frac{M}{D}}$ (s^{-1}) in (**Table 5**, **Table 6** with **Figure 1**) shows that the rate produce s will be increase with increasing coupling between NTCDA and Ag, the lowest $\mathcal{R}_{\frac{M}{D}}$ at every value of VDA with (ACN) solvent has the highest reorganization energy.

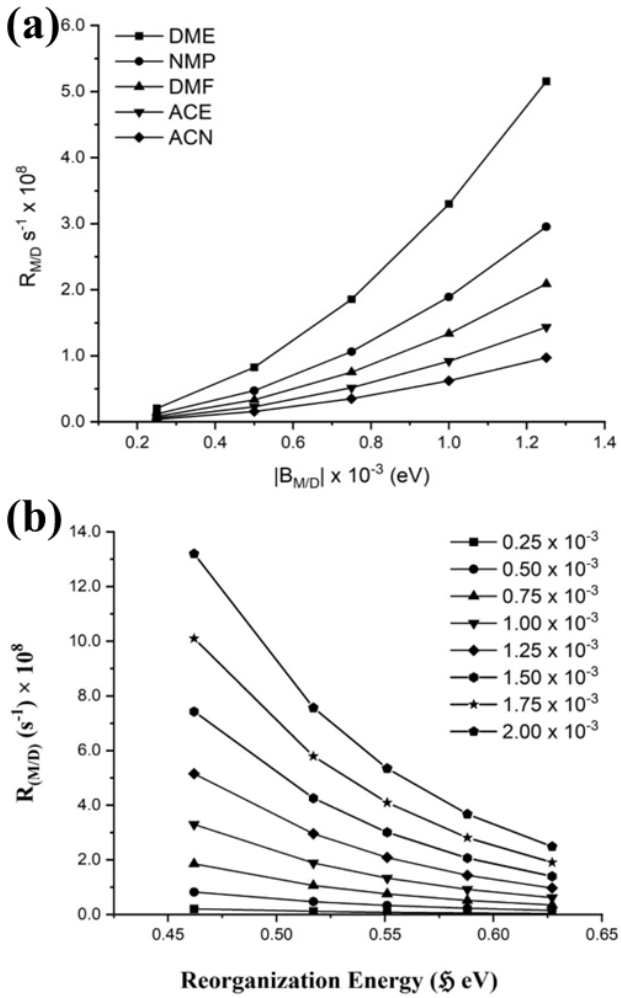


Figure 2. The charge transfer Rate Constants $\mathcal{R}_{\frac{M}{D}}$ (s^{-1}) for the Ag–NTCDA System as function of strength coupling (a) and reorganization energy(b).

The information shown in **Tables 5**, **6** and **Figures 1**, **2** show that electronic coupling between the Ag surface and NTCDA molecule is a crucial factor in determining the CT rate, in addition to the solvent effect. For each solvent (DME, NMP, DMF, ACE, and ACN) studied, the transfer rate significantly increased as the electronic coupling coefficient increased. The Fermi golden rule, which states that the transfer rate is directly proportional to the square of the ($\left|B_{\frac{M}{D}}\right|^2$) value, is consistent with this observation. The present results show that, rather than a single electronic characteristic, the CT rate dynamics at the Ag–NTCDA interface are affected by several linked parameters. The driving force for the transfer process, electronic coupling between the metal and the molecule, reorganization energy resulting from the rearrangement of the surrounding medium, and the effect of temperature on the occupancy of metallic electronic states are some of these parameters. The

Downloaded from https://nanomatimp.uomustansiriyah.edu.iq/

Copyright © 2026. This work licensed under a Creative Commons Attribution Noncommercial 4.0 International License.

results show that the effectiveness of CT in metal-molecule systems depends on a careful balance between promoting CT and providing the energy needed for system rearrangement after transfer. This relationship was clearly evidenced by the observed increase in the transfer rates when the electronic coupling coefficient was elevated from (0.25×10^{-3}) *to* (2.0×10^{-3}) eV. The maximum CT rate was observed at an electronic coupling coefficient of (2.0×10^{-3}) eV, ranging from $(1.168 \times 10^{9}$ *to* $1.168 \times 10^{9})(s^{-1})$ at 305 K and 315 K for all solvents. The results of charge transfer rate behavior agree with experimental results (from 5.68× 10^{7} 1/sec to 1.11 × 10^{8} 1/sec for system with Toluene solvent and from 3.13 × 10^{8}1/sec to 3.57 × 10^{8} 1/sec for system with Benzonitrile solvent[32, 33].

The results indicate that enhancing the electronic coupling between the metal (Ag) and the molecule (NTCDA) constitutes an effective strategy for augmenting charge transfer. This trend is consistent with the theory of non-adiabatic charge transfer, in which quantum considerations are combined with the electronic coupling constant and the density of acceptable states, weighted by the Franck-Condon factor, to determine the transfer rate. The data presented in Tables 5 and 6 demonstrate that an increase in the reorganization energy corresponds to a decrease in the CT rate, and vice versa.

The results further indicate that temperature (T) has a direct impact on the kinetics of CT at the Ag–NTCDA interface. This resulted an increasing the temperature from (305 to 315)K led to a 13–19% promotion in $\mathcal{R}_{\frac{M}{D}}$ across all solvents. For instance, in DME at $\left|B_{\frac{M}{D}}\right|^2 = 1.00 \times 10^{-3} eV$, the CT rate increases from 2.920×10^{8} to $3.299 \times 10^{8}\, s^{-1}$. This moderate increase is attributed to the interplay between the coefficient $(4\pi\hbar k_B T)^{\frac{-1}{2}}$ and the correction term $[1 - \frac{\pi^2 k_B T}{16\hbar}]$, as the occupation of the Fermi–Dirac states near E_F expand. The influence of temperature encompasses not only the enhancement of nuclear fluctuations but also the alteration of the availability of electronic states that participate in charge transfer. These patterns are consistent with prior Marcus-based research on dye and quantum systems, which demonstrated that the rate increased with enhanced coupling and decreased as the reorganization energy increased[12, 20, 28].

Conclusion

In this work, the Ag-NTCDA system was studied using a non-adiabatic system and quantum theory, and the Picard Factor (solvent polarity), reorganization energy, and charge transfer rate were estimated theoretically using the MATLAB implementation of the proposed model. The results indicate that the Picard coefficient plays a significant role in determining both the reorganization energy and CT rate. The reorganization energy values were between 0.462 and 0.627 depending on the solvent. When the reorganization energy decreased, the charger transfer increased to transfer from the Ag donor to the NTCDA molecule Accepter. In additional effect on increasing of charger transfer in the Ag - NTCDA interface when the electronic coupling increasing, the highest CT rate was achieved for DME with electronic coupling of (0.25-2) × 10^{-3}eV, whereas ACN solvent with 0.25 exhibited the lowest rate. The CT rate of Ag metal upon contact with NTCDA increases with temperature due to the increased kinetic energy of the electrons and decreased rearrangement energy, as described by Marcu's theory. Increasing the temperature in 305K and 315K enhanced the CT rate by approximately 13-19% depending on the solvent. These results suggest that the CT efficiency at metal–molecule interfaces are controlled by the combined effects of electronic coupling, solvent-dependent reorganization energy, and temperature, requiring a unified treatment in accordance with Marcu's theory.

Acknowledgment

Non.

Statement on Data Availability

All data, including simulation files supporting the study's conclusions, are available with either in the paper or you cand contact the author.

Declaration of Competing Interests

The author states that there are no conflicts of interest about this article.

Funding

The authors declare that no any funding was received for this study.

References

[1] A. Stefancu, N. J. Halas, P. Nordlander, and E. Cortes, "Electronic excitations at the plasmon–molecule interface," *Nature Physics*, vol. 20, no. 7, p. 1065–1077, 2024.

https://doi.org/10.1038/s41567-024-02537-6.

[2] Y. Wang and W. Dou, "Electron Transfer at Molecule-Metal Interfaces under Floquet Engineering: Rate Constant and Floquet Marcus Theory," *ACS Phys Chem Au*, vol. 4, no. 2, p. 160–166, 2024.

https://doi.org/10.1021/acsphyschemau.3c00049.

[3] R. Tonner, P. Rosenow, and P. Jakob, "Molecular structure and vibrations of NTCDA monolayers on Ag(111) from density-functional theory and infrared absorption spectroscopy," *Phys Chem Chem Phys*, vol. 18, no. 8, p. 6316–28, 2016.

https://doi.org/10.1039/c5cp06619k.

[4] P. Jakob *et al.*, "Adsorption geometry and interface states: Relaxed and compressed phases of NTCDA/Ag(111)," *Physical Review B*, vol. 94, no. 12, p. 125436–125436, 2016.

https://doi.org/10.1103/PhysRevB.94.125436.

Downloaded from https://nanomatimp.uomustansiriyah.edu.iq/

Copyright © 2026. This work licensed under a Creative Commons Attribution Noncommercial 4.0 International License.

[5] P. Rosenow, P. Jakob, and R. Tonner, "Electron-Vibron Coupling at Metal-Organic Interfaces from Theory and Experiment," *J Phys Chem Lett*, vol. 7, no. 8, p. 1422–7, 2016.

https://doi.org/10.1021/acs.jpclett.6b00299.

[6] R. A. Marcus, "Electron transfer reactions in chemistry. Theory and experiment," *Reviews of Modern Physics*, vol. 65, no. 3, p. 599–610, 1993.

https://doi.org/10.1103/RevModPhys.65.599.

[7] M. Zhang, Y. Chen, M. M. Melander, and J. Huang, "Electrochemical Electron Transfer: Key Concepts, Theories, and Parameterization via Atomistic Simulations," *Chem Rev*, vol. 126, no. 13, p. 7407–7464, 2026.

https://doi.org/10.1021/acs.chemrev.5c00926.

[8] A. Nitzan, "Electron transmission through molecules and molecular interfaces," *Annu Rev Phys Chem*, vol. 52, p. 681–750, 2001.

https://doi.org/10.1146/annurev.physchem.52.1.681.

[9] S. Maroo *et al.*, "Electronic origin of reorganization energy in interfacial electron transfer," *Nature*, vol. 653, no. 8113, p. 98–103, 2026.

https://doi.org/10.1038/s41586-026-10311-2.

[10] Q. R. Loague *et al.*, "Structural Gating Enhances Long-Distance Light-Driven Interfacial Electron Transfer," *ACS Cent Sci*, vol. 10, no. 11, p. 2132–2144, 2024.

https://doi.org/10.1021/acscentsci.4c01106.

[11] C. Reichardt and T. Welton, *Solvents and Solvent Effects in Organic Chemistry*, 4th, updated and enlarged ed. Weinheim: Wiley-VCH, 2010.

https://doi.org/10.1002/9783527632220.

[12] Z. Xi, "Revisiting the Marcus inverted regime: modulation strategies for photogenerated ultrafast carrier transfer from semiconducting quantum dots to metal oxides," *RSC Adv*, vol. 15, no. 33, p. 26897–26918, 2025.

https://doi.org/10.1039/d5ra04311e.

[13] F. Coppola, P. Cimino, U. Raucci, M. G. Chiariello, A. Petrone, and N. Rega, "Exploring the Franck-Condon region of a photoexcited charge transfer complex in solution to interpret femtosecond stimulated Raman spectroscopy: excited state electronic structure methods to unveil non-radiative pathways," *Chem Sci*, vol. 12, no. 23, p. 8058–8072, 2021.

https://doi.org/10.1039/d1sc01238j.

[14] D. Tannor, *Introduction to quantum mechanics: a time-dependent perspective*. MIT Press, 2008.

[15] O. Kühn and V. May, *Charge and Energy Transfer Dynamics in Molecular Systems*, 4th ed. Weinheim: Wiley-VCH, 2023.

https://doi.org/10.1002/9783527696277.

[16] D. J. Griffiths and D. F. Schroeter, *Introduction to Quantum Mechanics*, 3rd ed. Cambridge: Cambridge University Press, 2018.

https://doi.org/10.1017/9781316995433.

[17] M. Bixon and J. Jortner, "Electron Transfer—from Isolated Molecules to Biomolecules," in *Advances in Chemical Physics*, vol. 106(Advances in Chemical Physics: Wiley, 1999, pp. 35–202.

https://doi.org/10.1002/9780470141656.ch3.

[18] D. Ferry, *Quantum mechanics: an introduction for device physicists and electrical engineers*. CRC Press, 2020.

https://doi.org/10.1201/9781003031949.

[19] A. Nitzan, *Chemical Dynamics in Condensed Phases*, 2nd ed. Oxford: Oxford University Press, 2024.

https://doi.org/10.1093/9780191947971.001.0001.

[20] M. J. Fahimi, D. Fathi, M. Eskandari, and N. Das, "Marcus Theory and Tunneling Method for the Electron Transfer Rate Analysis in Quantum Dot Sensitized Solar Cells in the Presence of Blocking Layer," *Micromachines (Basel)*, vol. 14, no. 9, p. 1731–1731, 2023.

https://doi.org/10.3390/mi14091731.

[21] Y. Q. Gao and R. A. Marcus, "On the theory of electron transfer reactions at semiconductor/liquid interfaces. II. A free electron model," *The Journal of Chemical Physics*, vol. 113, no. 15, p. 6351–6360, 2000.

https://doi.org/10.1063/1.1309528.

[22] M. Z. Bazant, "Unified quantum theory of electrochemical kinetics by coupled ion-electron transfer," *Faraday Discuss*, vol. 246, no. 0, p. 60–124, 2023.

https://doi.org/10.1039/d3fd00108c.

[23] Y.-P. Liu and M. D. Newton, "Reorganization Energy for Electron Transfer at Film-Modified Electrode Surfaces: A Dielectric Continuum Model," *The Journal of Physical Chemistry*, vol. 98, no. 29, p. 7162–7169, 2002.

https://doi.org/10.1021/j100080a011.

[24] N. A. Sabri, M. A. Hassooni, H. J. M. Al-Agealy, and H. Kahtan, "Study of the efficiency of N719 dye-sensitized solar cells with cadmium selenide (cdse) semiconductor," *The European Physical Journal Plus*, vol. 141, no. 7, 2026.

https://doi.org/10.1140/epjp/s13360-026-08065-x.

[25] H. J. M. Al-agealy, K. H. Harbbi, M. A. Hassooni, and R. I. Noori, "Theoretical Study of Charge Transfer in Styryl Thiazilo Quinoxaline Dyes STQ-1, STQ-2,and STQ-3 in Organic Media System," *Baghdad Science Journal*, vol. 10, no. 4, p. 1262–1268, 2013.

https://doi.org/10.21123/bsj.2013.10.4.1262-1268.

[26] D. W. H. Rankin, "CRC handbook of chemistry and physics, 89th edition, edited by David R. Lide," *Crystallography Reviews*, vol. 15, no. 3, p. 223–224, 2009.

https://doi.org/10.1080/08893110902764125.

[27] S. A. Pshenichnyuk and A. S. Komolov, "Relation between electron scattering resonances of isolated

Downloaded from https://nanomatimp.uomustansiriyah.edu.iq/

Copyright © 2026. This work licensed under a Creative Commons Attribution Noncommercial 4.0 International License.

NTCDA molecules and maxima in the density of unoccupied states of condensed NTCDA layers," *J Phys Chem A*, vol. 116, no. 1, p. 761–6, 2012.

https://doi.org/10.1021/jp210224j.

[28] H. J. Al-Agealy and A. A. Al-Saadi, "Theory and Calculation of the Reorganization Energy of Electron Transfer at Liquid/Liquid Interface," *Ibn AL-Haitham Journal For Pure and Applied Science*, vol. 26, no. 2, p. 104–111, 2017.

[29] M. S. Ravenscroft and H. O. Finklea, "Kinetics of electron transfer to attached redox centers on gold electrodes in nonaqueous electrolytes," *The Journal of Physical Chemistry*, vol. 98, no. 14, p. 3843–3850, 2002.

https://doi.org/10.1021/j100065a047.

[30] C. De Luca, C. Giomini, and L. Rampazzo, "The multi-step reversible reduction of 1,4,5,8-naphthalene tetracarboxylic acid dianhydride," *Journal of Electroanalytical Chemistry and Interfacial Electrochemistry*, vol. 280, no. 1, p. 145–157, 1990.

https://doi.org/10.1016/0022-0728(90)87090-7.

[31] Y. Ai, Y. Liu, T. Cui, and K. Varahramyan, "Thin film deposition of an n-type organic semiconductor by ink-jet printing technique," *Thin Solid Films*, vol. 450, no. 2, p. 312–315, 2004.

https://doi.org/10.1016/j.tsf.2003.11.187.

[32] M. L. Williams, A. F. Coleman, K. R. Peinkofer, R. M. Young, and M. R. Wasielewski, "Structure-enabled long-lived charge separation in single crystals of an asymmetric donor-acceptor perylenediimide cyclophane," *Chem Sci*, vol. 15, no. 29, p. 11472–11479, 2024.

https://doi.org/10.1039/d4sc03359k.

[33] E. Sucre-Rosales, R. J. Fernandez-Teran, H. H. Huang, T. Solomek, and E. Vauthey, "Detecting photoinduced symmetry-breaking charge separation with near-zero driving force in a perylene diimide cage," *Phys Chem Chem Phys*, vol. 28, no. 32, p. 19746–19753, 2026.

https://doi.org/10.1039/d6cp02527g.

Downloaded from https://nanomatimp.uomustansiriyah.edu.iq/

Copyright © 2026. This work licensed under a Creative Commons Attribution Noncommercial 4.0 International License.